

Effect of hydroxyl bonds on persistent spectral hole burning in Eu^{3+} -doped $\text{BaO-P}_2\text{O}_5$ glasses

Masayuki Nogami,* Naoto Umehara, and Tomokatsu Hayakawa
Nagoya Institute of Technology, Showa Nagoya, 466-8555 Japan
 (Received 16 April 1998)

The effect of OH bonds on the optical absorption and persistent spectral hole burning (PSHB) properties was quantitatively analyzed in Eu^{3+} -doped $\text{BaO-P}_2\text{O}_5$ glasses. Glasses were prepared by melting the raw material at 600–800 °C, in which the OH content was changed. The hole was burned in the ${}^7F_0 \rightarrow {}^5D_0$ transition of the Eu^{3+} ions at 6 K and the dependence of the PSHB properties on temperature and time was measured. The bond covalency between Eu^{3+} and oxygens decreased and the hole depth linearly increased with increasing the OH content in the glass. The proposed model was that the hole was burned by the optically activated rearrangement of the OH bonds surrounding the Eu^{3+} ions. The hole burnt at 6 K was refilled with increasing time and temperature and an average thermal barrier height for the hole filling was ~ 140 meV, which was smaller than that for the Eu^{3+} ions doped in silica and silicate glasses. [S0163-1829(98)06834-9]

I. INTRODUCTION

The persistent spectral hole burning (PSHB) phenomenon of Eu^{3+} and Sm^{2+} ions is one of the most significant optical properties for use in high-density frequency-domain optical data memory,¹ and thus many studies have been carried out to develop the PSHB materials. Macfarlane and Shelby first found the hole burning for the Eu^{3+} ion-doped glasses at liquid-helium temperatures.² For practical use, high-temperature PSHB is required. So far, the PSHB at temperatures using liquid nitrogen has been observed in the Eu^{3+} -doped β'' -alumina³ and silicate glasses.⁴ Further room-temperature PSHB has been observed in the Sm^{2+} ions doped in crystals⁵ and glasses.^{6,7} As a host material, glasses are thought to be more favorable than crystals, because of their wide inhomogeneous width, compositional variety, and easy mass production. We have been conducting a study of the preparation of the PSHB glasses by use of a sol-gel method, and recently succeeded in preparing aluminosilicate glasses doped with Sm^{2+} and Eu^{3+} ions exhibiting PSHB up to 300 and 210 K, respectively.^{8–10} Since the Eu^{3+} -doped glasses are obtained without heating in reducing atmosphere, it thus becomes possible to extend the study beyond the limitation of the Sm^{2+} -doped glasses.

Eu^{3+} and Sm^{2+} ions have the same electron configuration $4f^6$, the lowest and first excited states of which are 7F_0 and 5D_0 , respectively. The holes are burned on the excitation spectra of the ${}^7F_0 \rightarrow {}^5D_0$ transition of the Eu^{3+} and Sm^{2+} ions though the burning mechanism seems to be quite different. A possible main reaction for hole burning in the Sm^{2+} ions is the photoionization of Sm^{2+} into Sm^{3+} by laser irradiation,¹¹ although the question of where the produced electrons are captured still remains unknown. On the other hand, the Eu^{3+} ions are stable, not to be ionized by laser beam. In a previous paper, we found that in the sol-gel glasses the hole depth proportionally increased as the residual water content increased,¹² and thus the sol-gel technique is appropriate to prepare the PSHB materials with high resolution for data storage. These results suggest that the PSHB can be observed in the glasses prepared by the con-

ventional melt quenching if they contain the OH bonds together with the Eu^{3+} ions.

This paper presents the PSHB properties for the Eu^{3+} -doped $\text{BaO-P}_2\text{O}_5$ glasses that are prepared by the melting method. The local structure around the Eu^{3+} ions is studied using the Judd-Ofelt parameters and the fluorescence line-narrowing spectra. We discuss how the OH bonds surrounding the Eu^{3+} ions contribute to the hole burning from the experimental data of hole refilling.

II. EXPERIMENT

$3\text{BaO} \cdot 7\text{P}_2\text{O}_5$ glasses doped with 1 mol % Eu_2O_3 were prepared by melting mixture of reagent grade BaCO_3 , H_3PO_4 , and Eu_2O_3 for 2 h at 600 to 800 °C in an alumina crucible. Each melt was then cast in a graphite mold and annealed at 300 °C for 10 min. Glasses were cut to 3-mm thickness and polished for the optical measurements. A possible small change in the glass composition caused by vaporization during melting is neglected except for the residual water.

Optical absorption spectra of Eu^{3+} were recorded in the wavelength range of 300 to 600 nm at room temperature. Three Judd-Ofelt parameters $\Omega_t (t=2,4,6)$ were determined by using the integrated absorbance and the equation^{13,14}

$$(4.32 \times 10^{-9}) \int \alpha(\nu) d\nu = \frac{8\pi^2 m c \nu}{3h(2J+1)} \frac{(n^2+2)^2}{9n} \sum_{t=2,4,6} \Omega_t \langle aJ \| U^{(t)} \| bJ' \rangle^2, \quad (1)$$

where $\alpha(\nu)$ is the measured molar absorption coefficient at a given wave number ν , h is Planck's constant, m is the mass of electron, c is the speed of light, n is the refractive index, and $\langle aJ \| U^{(t)} \| bJ' \rangle$ is the reduced matrix elements of the unit tensor operator for the corresponding transition.

Low-resolution fluorescence spectra were measured at room temperature. The 337-nm light of the N_2 laser was used as pumping source for excitation of the Eu^{3+} ion. For the fluorescence lifetime measurements, the N_2 laser with nsec

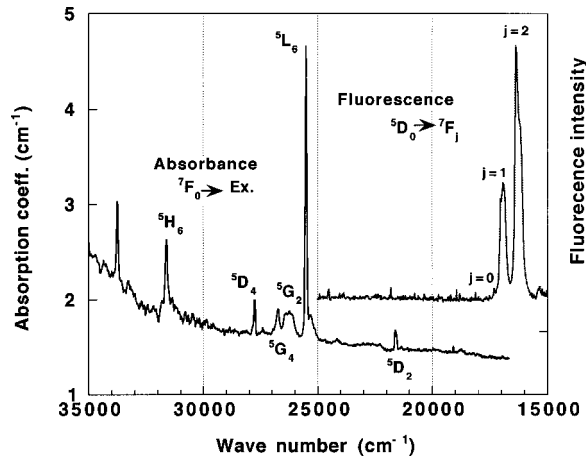


FIG. 1. Optical absorption and fluorescence spectra, measured at room temperature, of Eu^{3+} -doped $3\text{BaO}\cdot 7\text{P}_2\text{O}_5$ glass melted at 600°C . The fluorescence spectrum was obtained with the $2.97 \times 10^4\text{-cm}^{-1}$ excitation wavelength of a N_2 laser. The energy states shown in figure are transitions from the ground state 7F_0 .

resolution was focused onto the sample and the fluorescence spectra were recorded using a CCD camera at 0.01-msec intervals after turning off the laser irradiation. The fluorescence line narrowing (FLN) measurement was performed under excitation with a wavelength within the ${}^7F_0 \rightarrow {}^5D_0$ transition by a rhodamine 6G dye laser. The fluorescence intensity was measured with a chopper that alternately opened the optical paths before and after the sample. The chopping frequency was 150 Hz. All FLN spectra were recorded at 6 K with the Jobin Yvon HR 320 monochromator.

The PSHB was observed on the excitation spectrum of the ${}^7F_0 \rightarrow {}^5D_0$ transition of the Eu^{3+} . The excitation spectrum was obtained by scanning the output of a cw Ar^+ -ion laser-pumped rhodamine 6G dye laser with a linewidth of $\sim 1.0\text{ cm}^{-1}$ full width at half maximum (FWHM) from $17\,100$ to $17\,550\text{ cm}^{-1}$ while monitoring the fluorescence of the ${}^5D_0 \rightarrow {}^7F_2$ transition at $16\,260\text{ cm}^{-1}$. The glass was then irradiated using a rhodamine 6G dye laser with a spot size of about 1 mm diam operating at 300 mW for 30 min. After irradiation, the excitation spectrum was recorded in the same way. The laser power for scanning was attenuated by neutral-density filters to less than 0.2% of that for burning.

Infrared spectra were obtained between 4000 and 1500 cm^{-1} for the $0.05\text{--}0.1\text{-mm}$ -thick sample.

III. RESULTS

A. Absorption properties

The room-temperature absorption spectrum for the glass melted at 600°C is shown in Fig. 1. The absorption spectrum consists of several electric transitions from the 7F_0 ground state to the excited states shown in the figure. Similar spectra were obtained for glasses obtained by melting at 700 and 800°C , the transition energies of which are similar to those observed for many Eu^{3+} ion-doped oxide glasses such as silicate,¹⁵ borate,¹⁶ and phosphate.^{17,18} The Judd-Ofelt parameters $\Omega_{t(t=2,4,6)}$ are characteristic of the rare-earth ions in the matrix and are used to characterize the environmental field of the rare-earth ions. The parameter Ω_2 is related to the

TABLE I. Optical absorption (Judd-Ofelt parameters) and fluorescence (decay time and intensity ratio of ${}^5D_0 \rightarrow {}^7F_2$ to ${}^5D_0 \rightarrow {}^7F_1$) properties of Eu^{3+} -doped $3\text{BaO}\cdot 7\text{P}_2\text{O}_5$ glasses.

Melting temperature ($^\circ\text{C}$)	Ω_2 ($\times 10^{-20}\text{ cm}^2$)	Ω_4 ($\times 10^{-20}\text{ cm}^2$)	Ω_6 ($\times 10^{-20}\text{ cm}^2$)	Decay time (msec)	Intensity ratio
600	3.72	4.15	2.01	2.00	2.67
700	4.53	3.30	1.91	2.10	3.08
800	4.31	3.13	1.52	2.24	3.19

covalency and structural change in the vicinity of the Eu^{3+} ion and Ω_4 is related to the long-range effects. Ω_6 tends to increase with decreasing rigidity of the surrounding medium. The best fit of parameters $\Omega_{t(t=2,4,6)}$ determined by the method of least-squares analysis using Eq. (1) are listed in Table I. There exists an increasing tendency of parameter Ω_2 and the decrease in both the Ω_4 and Ω_6 with increasing the melting temperature. These results are ascribed to the increased covalency of the chemical bond between the Eu^{3+} ion and the neighboring oxygens in glass melted at high temperature.

B. Fluorescence properties

As shown in Fig. 1, which illustrates the fluorescence spectrum using the $2.97 \times 10^4\text{ cm}^{-1}$ (337-nm) excitation wavelength of a N_2 laser, three broadened lines are observed at $\sim 17\,200$, $\sim 16\,900$, and $\sim 16\,300\text{ cm}^{-1}$ in the visible region, which are attributed to transitions from 5D_0 to 7F_0 , 7F_1 , and 7F_2 states in order of increasing wavelength, respectively, of the Eu^{3+} ions. The ${}^5D_0 \rightarrow {}^7F_1$ transition is a magnetic dipole transition, and hardly varies with the crystal-field strength around the Eu^{3+} ion. On the other hand, the ${}^5D_0 \rightarrow {}^7F_0$ and 7F_2 transitions are electric dipole ones and are sensitive to chemical bonds in the vicinity of Eu^{3+} ion, that is, the fluorescence intensities are enhanced when the chemical bond between the Eu^{3+} and oxygens become more covalent. Therefore, the intensity ratio of the ${}^5D_0 \rightarrow {}^7F_2$ (or 7F_0) transition to the ${}^5D_0 \rightarrow {}^7F_1$ transition can be used to estimate the chemical bond surrounding the Eu^{3+} ions. The intensity ratio of the ${}^5D_0 \rightarrow {}^7F_2$ transition to the ${}^5D_0 \rightarrow {}^7F_1$ transition for the glasses prepared by melting at $600\text{--}800^\circ\text{C}$ is presented in Table I. A large value of the intensity ratio is observed for the glass melted at high temperature, indicating that a strong Eu-O bond is formed in the glasses.

The laser-induced fluorescence line-narrowing spectroscopy is more useful to study the local environment of the Eu^{3+} ion. The FLN spectra were measured at 6 K after excitation at different energies inside the ${}^7F_0 \rightarrow {}^5D_0$ transition. Figure 2 shows typical spectra for the glasses prepared by melting at 600 and 800°C under excitation at the wavelength of the center within the ${}^7F_0 \rightarrow {}^5D_0$ transition. The spectra of the ${}^5D_0 \rightarrow {}^7F_1$ and 7F_2 transitions have three and five distinct peaks, respectively, due to the Stark splitting of these states. To study the Stark splitting of each state, the spectra of the ${}^5D_0 \rightarrow {}^7F_1$ and 7F_2 transitions were deconvoluted using the Gaussian distribution function. A fit is shown in Fig. 2, indicating that the 7F_1 and 7F_2 states consist of

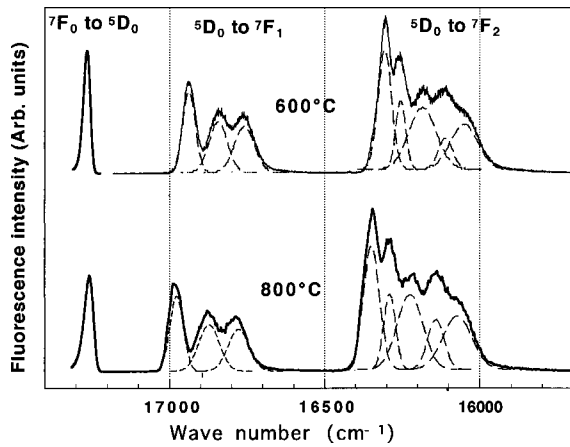


FIG. 2. Fluorescence and excitation spectra, measured at 6 K, of Eu^{3+} -doped $3\text{BaO}\cdot 7\text{P}_2\text{O}_5$ glasses melted at 600 and 800 °C. The fluorescence spectra were obtained using excitation with the centered energy within the ${}^7F_0 \rightarrow {}^5D_0$ transition band. The excitation spectra were obtained by monitoring the ${}^5D_0 \rightarrow {}^7F_2$ fluorescence at $16\,260\text{ cm}^{-1}$.

three and five components, respectively. No additional fluorescence bands were observed when the excitation energy was changed within the ${}^7F_0 \rightarrow {}^5D_0$ transition. These results indicate that the Eu^{3+} ions at different sites in a matrix have the same type of ligand structure, but are not located in the different phases observed in the same glasses doped with Eu^{3+} ions.¹⁹ The difference in energy between the positions of an individual component and the excitation energy is plotted in Fig. 3 as a function of excitation energy for the glasses melted at 600 and 800 °C. The values determined for glasses prepared by melting at 700 °C (not plotted for clarification) are similar to those shown in Fig. 3. It is found that the peak positions of these transitions manifest systematic shifts when the ${}^7F_0 \rightarrow {}^5D_0$ excitation energy is changed. Since the ${}^7F_0 \rightarrow {}^5D_0$ excitation energy is a measure of the strength of the crystal field acting on central Eu^{3+} ions, such spectral shift

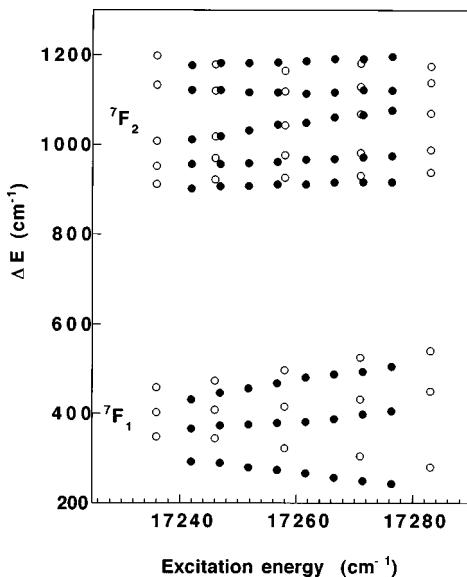


FIG. 3. Energy difference between the peak energies of the deconvoluted ${}^5D_0 \rightarrow {}^7F_{1,2}$ transition lines and the excitation energy in glasses melted at 600 °C (open circles) and 800 °C (closed circles).

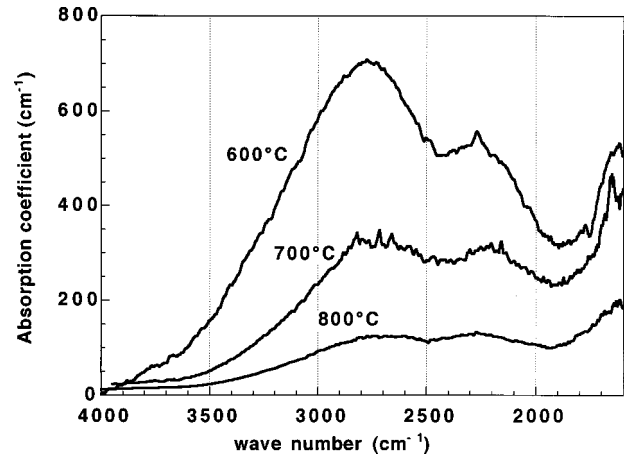


FIG. 4. Infrared spectra of Eu^{3+} -doped $3\text{BaO}\cdot 7\text{P}_2\text{O}_5$ glasses melted at 600, 700, and 800 °C.

can be attributed to the variation of the local crystal-field strength of the Eu^{3+} ions in glass.²⁰ Among the three lines of the 7F_1 state, the lowest-energy line shifts remarkably to lower energies with an increase of the ${}^7F_0 \rightarrow {}^5D_0$ excitation energy, while the other two lines shift to higher energies.

The ${}^7F_0 \rightarrow {}^5D_0$ transition is a nondegenerate transition, the width of which is the measurement of the site distribution surrounding the Eu^{3+} ion. The band, obtained by scanning the rhodamine 6G dye laser while monitoring the fluorescence of the ${}^5D_0 \rightarrow {}^7F_2$ transition at $16\,260\text{ cm}^{-1}$, exhibits a width of about 25–35 cm^{-1} FWHM (see Fig. 2), which is narrower than half of that observed for the metaphosphate glasses.¹⁷

C. Infrared-absorption spectra

Characteristic of the phosphate glasses is the fact that a large amount of water remains in them in comparison to the silicate glasses. Water in glass was investigated by infrared spectroscopy; spectra for glasses melted at 600–800 °C are shown in Fig. 4. Broad absorption bands having peaks at ca. 2800 and 2200 cm^{-1} are observed, the former of which is assigned to the fundamental stretching vibrations of OH groups. In contrast, the broadband at 2200 cm^{-1} is overlapped with various bands due to P-O-P and H_2O , which makes the assignment difficult. Day and Stevls found out that the 2920- cm^{-1} band exhibits an increase proportional to the content of the P-OH bonds.²¹ To clarify the P-OH bonds in our glasses, the IR spectra were deconvoluted, using Gaussian functions, into two bands peaking at ca. 2800 and 2200 cm^{-1} , and the absorption coefficients of the 2800- cm^{-1} band are listed in Table II. Note that the absorption coefficient of the 2800- cm^{-1} band drastically decreases with increasing the melting temperature.

D. Persistent spectra hole burning

PSHB was observed on the excitation spectra of the ${}^7F_0 \rightarrow {}^5D_0$ transition. Figure 5 shows a typical excitation spectra before and after hole burning at 6 K with laser with a power of 300 mW at $17\,265\text{ cm}^{-1}$ for 30 min. The PSHB spectrum was recorded after 30 min of turning off the laser. A hole is clearly observed at the burning wave number of

TABLE II. PSHB (hole depth and area) properties and infrared-absorption coefficient at 2800 cm^{-1} of Eu^{3+} -doped $3\text{BaO}\cdot 7\text{P}_2\text{O}_5$ glasses.

Melting temperature ($^{\circ}\text{C}$)	Absolute coefficient of 2800-cm^{-1} band (cm^{-1})	Hole depth (%)	Hole area
600	450	44	0.0210
700	250	23	0.0105
800	40	10	0.0046

$17\,265\text{ cm}^{-1}$. The width and depth of the burned hole are 1.0 cm^{-1} FWHM and 44% of the total fluorescence intensity, respectively. The values of depth and area of holes, burned and measured at 6 K, for glasses melted at 600 to $800\text{ }^{\circ}\text{C}$ are listed in Table II, in which the hole area is defined as the ratio of hole area to the total area of the ${}^7F_0 \rightarrow {}^5D_0$ transition band. It is evident that the hole becomes small with increasing the melting temperature. Further, it is interesting to notice that the increased fluorescence can be clearly observed around the hole (see the difference spectrum before and after laser irradiation in the inset of Fig. 5).

Figure 6 shows the multihole spectra, where six holes were burned in order increasing number for 30 min at 6 K. Note that the previously burned hole is partially refilled by the increased fluorescence around the new hole.

IV. DISCUSSION

A. Contribution of OH bonds to PSHB

In general, phosphate glasses are composed of a three-dimensional network structure of the PO_4 tetrahedron termi-

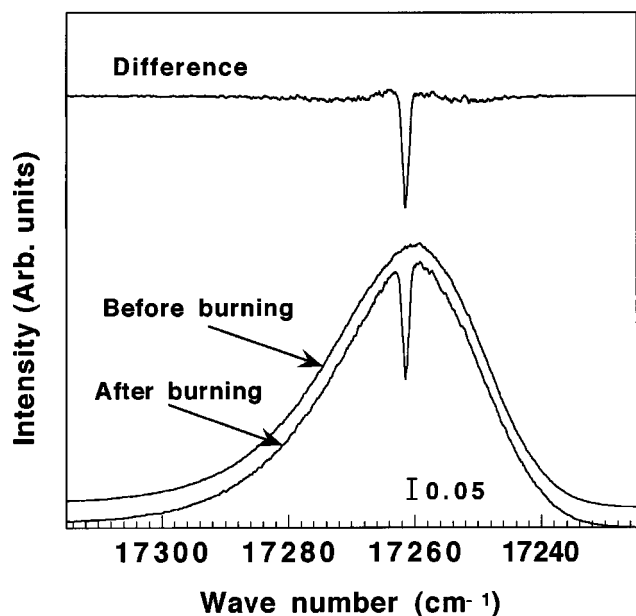


FIG. 5. Excitation spectra, measured at 6 K, of Eu^{3+} -doped $3\text{BaO}\cdot 7\text{P}_2\text{O}_5$ glasses melted at $600\text{ }^{\circ}\text{C}$ before and after hole burning. Burning power and time are 300 mW at $17\,265\text{ cm}^{-1}$ and 30 min, respectively. The spectrum before burning was moved by 0.05 in scale for clarification. The difference intensities between before and after burning are shown in the top spectrum.

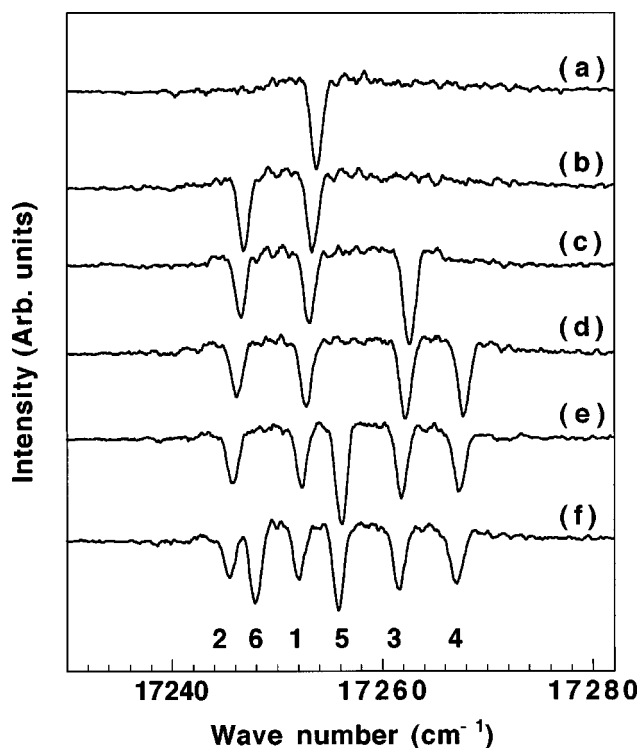


FIG. 6. Multihole spectra of Eu^{3+} -doped $3\text{BaO}\cdot 7\text{P}_2\text{O}_5$ glass. Holes were burned at six wave numbers in the order of numbers shown at 6 K.

nating with the modifier cations such as Ba^{2+} and Eu^{3+} ions,^{17,18} and a large amount of water remains in the glasses in comparison to the silicate glasses. H_2O in phosphate glasses forms OH groups bonding to P ions. The Eu^{3+} ions are considered to be surrounded by eight or nine oxygens that consist of the PO_4 tetrahedron. The Judd-Ofelt parameters have been successfully used in estimating the environment of the rare-earth ion. As shown in Tables I and II, the decrease in OH content causes the parameter Ω_2 to increase and the Ω_4 and Ω_6 parameters to decrease. These changes in the parameters indicate that the covalency of the chemical bond between the Eu^{3+} ion and the neighboring oxygens increases with decreasing the OH content. Since the P-OH bonds are more covalent than the P-O⁻ bonds, the electron-donating ability of oxygen in P-O⁻ bonds can be higher than that in P-OH bonds. This predominant factor that affects the field at the Eu^{3+} ion is that the covalency of the Eu-O bond is increased with decreasing the number of OH bonds surrounding the Eu^{3+} ions.

The effect of OH groups in the first coordination sphere of the Eu^{3+} ion can be also discussed from the measurement of the fluorescence decay behavior. A larger decay time for glasses melted at high temperature is shown in Table I. The presence of OH groups surrounding Eu^{3+} ion provides an effective pathway for the radiationless deexcitation via energy transfer to OH vibration that results in a shorter decay time and quenching of the fluorescence.²²

In the previous paper, we measured the PSHB of the Eu^{3+} -doped SiO_2 and $\text{Al}_2\text{O}_3\text{-SiO}_2$ glasses prepared by the sol-gel method and found that the hole depth increased with increasing the OH content.^{9,10,12} In these Eu^{3+} -doped SiO_2 and $\text{Al}_2\text{O}_3\text{-SiO}_2$ glasses, the H_2O molecules are bound with

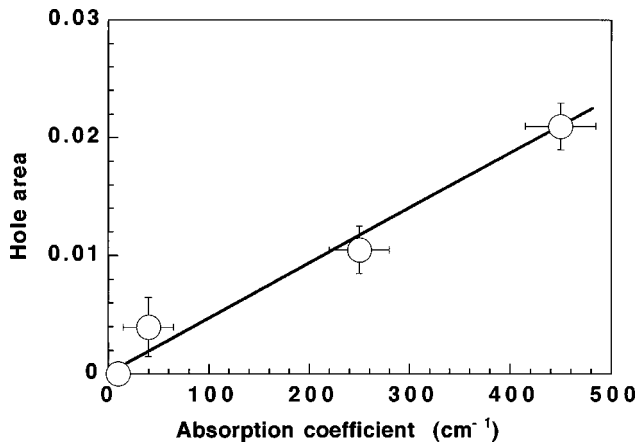


FIG. 7. Hole area as a function of the absorption coefficient of 2800 cm^{-1} band.

Eu^{3+} , Al^{3+} , and Si^{4+} ions to form the hydrogen-bonded OH groups. When the laser beam is irradiated, the protons in the OH groups bond with Eu^{3+} and/or the OH bonds and surrounding Eu^{3+} ions change their positions to form a different bonding feature. This rearrangement of the proton bonding can be considered to result in the hole burning. To elucidate the effect of the OH bonds on the hole burning in the present Eu^{3+} -doped $\text{BaO-P}_2\text{O}_5$ glasses the relation between the hole area and the absorption coefficient of the 2800-cm^{-1} band is plotted in Fig. 7, in which the hole area is defined as the ration of the hole area to the total area of the ${}^7F_0 \rightarrow {}^5D_0$ excitation band. Note that the hole area increases with increasing the absorption coefficient. This result indicates that the existence of the OH bonds surrounding the Eu^{3+} ions seems important for the hole burning, and we propose that the holes for the Eu^{3+} -doped phosphate glasses are burned by the rearrangement of OH bonds. The proposed reaction is schematically illustrated in Fig. 8. When the laser is irradiated, the protons in the OH groups surrounding Eu^{3+} ions (A site) change their positions to form a different bonding feature (B site). This rearrangement of the proton bonding results in the hole burning. These results clearly explain that the deep holes are burned in the glasses containing a large amount of OH bonds.

B. Refilling of hole

The hole-burnt state (state II) has a higher energy than the unburnt state (state I) and it relaxes across the activation barrier into the unburnt state as shown in Fig. 8. The stability of the hole-burnt state can be discussed from the temperature-dependent and time-dependent hole-erasure experiments. In this reaction, the optically activated state (state II in Fig. 8) relaxes across the activation barrier V into the unburnt state (state I), the rate of which is given as²²

$$R = R_0 \exp(-V/kT), \quad (2)$$

where R_0 is the attempt frequency, k is the Boltzmann constant, and T is the temperature in K. Assuming that the barrier height follows a Gaussian distribution and the fraction of the remaining hole F is proportional to the number of photoproducts of state II that remain unchanged, F is given as a function of time t as follows:

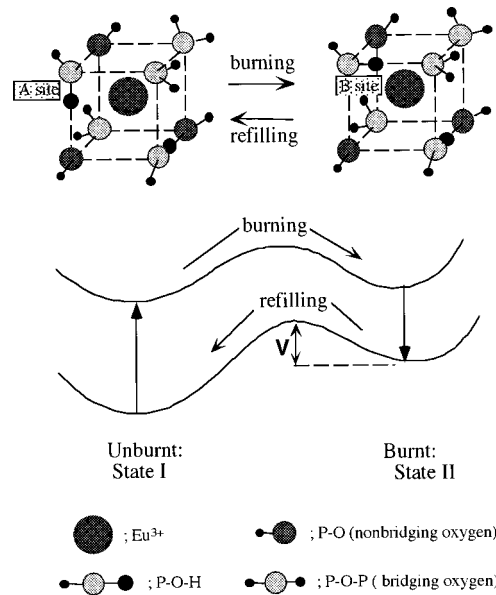


FIG. 8. Proposed hole burning model in Eu^{3+} -doped $3\text{BaO} \cdot 7\text{P}_2\text{O}_5$ glass. Hole is burned when the OH bonds in state I are changed from A to B site by light irradiation. State II has higher energy compared with the state I and relaxes across the barrier into the state I.

$$F(t) = \int_{-\infty}^{+\infty} g(V) \exp(-Rt) dV. \quad (3)$$

The fraction of the remaining hole is also presented as a function of the holding temperature T , higher than the burning temperature,

$$F(T) = 1 - \int_0^{kT \ln(R_0 t_0)} g(V) dV, \quad (4)$$

where t_0 is the holding time at temperature T . The dependence of hole area on temperature was investigated from the temperature-cycling experiment of the hole. A hole was formed at 6 K. After cycling through a certain temperature higher than the burning temperature, the spectra were again measured at 6 K. During this process, the hole might be partially filled. Figure 9 shows the hole area as a function of the cycling temperature, where the hole area is normalized to

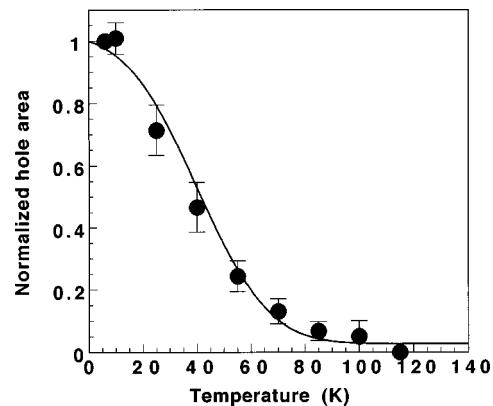


FIG. 9. Relation between the hole area and the cycling temperature of Eu^{3+} -doped $3\text{BaO} \cdot 7\text{P}_2\text{O}_5$ glass. The solid curves indicate a fit to data based on a Gaussian distribution function; see the text.

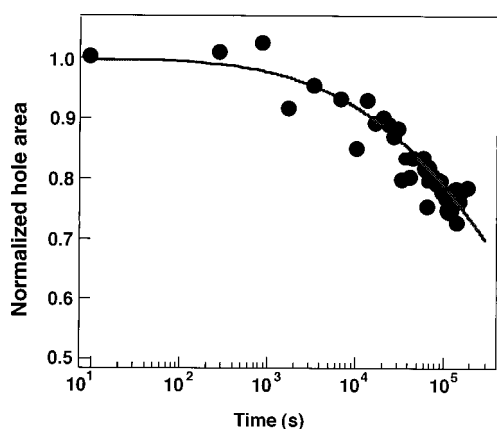


FIG. 10. Relation between the hole area and the time after burning of Eu^{3+} -doped $3\text{BaO}\cdot 7\text{P}_2\text{O}_5$ glass. The solid curves indicate a fit to data based on a Gaussian distribution function; see the text.

unity at 6 K. It is evident that the hole burned at 6 K decreases its area with an increase in the temperature, resulting in erasure above about 130 K. Also, the time dependence of the hole area at 6 K is plotted with logarithmic scale in Fig. 10, where the hole area is normalized to unity at 5 min after burning. Note that the hole keeps its area within 20 h and then decreases with increasing time. The solid curves shown in Figs. 9 and 10 are the fitting of the data using Eqs. (3) and (4), respectively, and the fitting parameters V are estimated to be ~ 140 meV for both data with $R_0 = 10^{14}$ sec^{-1} and $t = 1800$ sec. It is interesting to note that the obtained V is smaller than that for the Eu^{3+} ions doped in silica and silicate glasses.¹² The V value is a measure of the stability of

PSHB and is considered to be dependent on the strength of the OH bonds surrounding the Eu^{3+} ions. The OH groups bound to P^{5+} ions are hydrogen bonded with the Eu^{3+} ions, in which the hydrogen-bonding strength is strongly dependent on the bond strength between oxygen and cation such as P and Si. Compared with Si-OH bonds, the P-OH bonds are strongly hydrogen bonded with the Eu^{3+} ion and their OH bonds are easily changed by the small energy, resulting in the small V value. This is the reason for determining the temperature of PSHB and these data are instructive for developing the glasses exhibiting PSHB up to high temperatures.

V. CONCLUSIONS

In this paper, the PSHB was measured for the Eu^{3+} -doped $\text{BaO-P}_2\text{O}_5$ glasses prepared by the melt-quenching method. Depth of the hole, burned in the ${}^7F_0 \rightarrow {}^5D_0$ transition of the Eu^{3+} ions at 6 K, linearly increased with increasing the OH content in the glass and the burnt hole was refilled with increasing time and temperature. We concluded that spectral hole burning proceeds as an optically activated rearrangement of the OH bonds surrounding the Eu^{3+} ions and the hole stability in the phosphate glasses is small compared with the silicate glasses.

ACKNOWLEDGMENTS

This research was partly supported by a Grant-in-Aid for Scientific Research (No. 09650734) from the Ministry of Education, Science, and Culture of Japan.

*Electronic address: nogami@mse.nitech.ac.jp

¹G. Castro, D. Haarer, R. M. Macfarlane, and H. P. Trommsdorff, U.S. Patent No. 4,101,976 (July 1978).

²R. M. Macfarlane and R. M. Shelby, *Opt. Lett.* **9**, 533 (1984).

³H. Yugami, R. Yagi, S. Matsuo, and M. Ishigame, *Phys. Rev. B* **53**, 8283 (1996).

⁴Y. Mao, P. Gavrilovic, S. Singh, A. Bluce, and W. H. Grodkiewicz, *Appl. Phys. Lett.* **68**, 3677 (1996).

⁵R. Jaaniso and H. Bill, *Europhys. Lett.* **16**, 569 (1991).

⁶K. Hirao, S. Todoroki, D. H. Cho, and N. Soga, *Opt. Lett.* **18**, 1586 (1993).

⁷A. Kurita and T. Kushida, *Opt. Lett.* **19**, 314 (1994).

⁸M. Nogami, Y. Abe, K. Hirao, and D. H. Cho, *Appl. Phys. Lett.* **66**, 2952 (1995).

⁹M. Nogami and Y. Abe, *Appl. Phys. Lett.* **71**, 3465 (1997).

¹⁰M. Nogami and Y. Abe, *J. Opt. Soc. Am. B* **15**, 680 (1998).

¹¹A. Winnacker, R. M. Shelby, and R. M. Macfarlane, *Opt. Lett.* **10**, 350 (1985).

¹²M. Nogami and T. Hayakawa, *Phys. Rev. B* **56**, R14 235 (1997).

¹³W. T. Carnall, P. R. Fields, and B. G. Wybourne, *J. Chem. Phys.* **42**, 3797 (1963).

¹⁴B. R. Judd, *Proc. Phys. Soc. London, Sect. A* **69**, 157 (1956).

¹⁵T. F. Belliveau and D. J. Simkin, *J. Non-Cryst. Solids* **110**, 127 (1989).

¹⁶M. Bettinelli, A. Speghini, M. Ferrari, and M. Montagna, *J. Non-Cryst. Solids* **201**, 211 (1996).

¹⁷J. A. Capobianco, P. P. Proulx, M. Bettinelli, and F. Negrisolo, *Phys. Rev. B* **42**, 5936 (1990).

¹⁸K. Hirao, S. Todoroki, and N. Soga, *J. Non-Cryst. Solids* **175**, 263 (1994).

¹⁹G. Pucker, K. Gatterer, H. P. Fritzer, M. Bettinelli, and M. Ferrari, *Phys. Rev. B* **53**, 6225 (1996).

²⁰C. Brecher and A. Riseberg, *Phys. Rev. B* **13**, 81 (1976).

²¹D. E. Day and J. M. Stevls, *J. Non-Cryst. Solids* **11**, 459 (1973).

²²Z. Jiahua, H. Shihua, and Y. Jiaqi, *Opt. Lett.* **17**, 1146 (1992).